

Hyperinsulinemia and ectopic fat deposition can develop in the face of hyperadiponectinemia in young obese rats[☆]

John C. Marecki^{a,b}, Martin J.J. Ronis^{a,b,c}, Kartik Shankar^{a,b}, Thomas M. Badger^{a,b,d,*}

^aArkansas Children's Nutrition Center, Little Rock, AR 72202, USA

^bDepartment of Pediatrics, University of Arkansas for Medical Sciences, Little Rock, AR 72205, USA

^cDepartment of Pharmacology and Toxicology, University of Arkansas for Medical Sciences, Little Rock, AR 72205, USA

^dDepartment of Physiology and Biophysics, University of Arkansas for Medical Sciences, Little Rock, AR 72205, USA

Received 18 May 2009; received in revised form 22 December 2009; accepted 4 January 2010

Abstract

Serum adiponectin has been reported to inversely correlate with the degree of adiposity in children. However, the relative contribution of adiponectin-dependent signaling to the development of metabolic syndrome in childhood obesity is unclear. We overfed prepubertal, male Sprague–Dawley rats a high-fat diet via total enteral nutrition. Excessive caloric intake led to obesity, increased body weight and fat mass; dyslipidemia; ectopic fat deposition; and hyperinsulinemia ($P < .05$). Expression of fatty acid transporter FAT/CD36 was elevated in both liver and skeletal muscle ($P < .05$). Hepatic Akt phosphorylation was elevated ($P < .05$) and FoxO1 protein in hepatic nuclear extracts was reduced ($P < .05$) in the face of hyperinsulinemia, whereas no increase in Akt phosphorylation or decrease in nuclear FoxO1 was observed in skeletal muscle. Overfeeding increased serum adiponectin concentration from 24.6 ± 1.9 $\mu\text{g/ml}$ to 46.3 ± 5.9 $\mu\text{g/ml}$ ($P < .004$), and positively correlated with increased adipose tissue mass. The expression of the inflammatory cytokine tumor necrosis factor α in the adipose tissue was unchanged. Adiponectin-mediated adenosine monophosphate (AMP) kinase phosphorylation, peroxisome proliferator-activator receptor- α expression and the expression of genes involved in fatty acid oxidation were elevated in both liver and muscle ($P < .05$). These data (1) demonstrate that excessive intake of a high-fat diet in young rats results in “adiponectin-independent” increases in ectopic fat deposition and hyperinsulinemia, (2) suggest that fatty acid transport is a major mechanism underlying ectopic fat deposition, (3) demonstrate tissue-specific differences in the response of Akt-FoxO signaling to hyperinsulinemia following the development of pediatric obesity and (4) suggest age-related differences in the role of adiponectin in pathological responses associated with obesity. © 2011 Elsevier Inc. All rights reserved.

Keywords: Pediatric obesity; Non-alcoholic fatty liver disease; Adiponectin; Total enteral nutrition; High fat; FAT/CD36

1. Introduction

Childhood obesity is associated with the rapid rise in the prevalence of health complications that were once thought to be primarily adult disorders, such as Type 2 diabetes, cardiovascular disease and other sequelae of the “metabolic syndrome” [1]. Studies in children have shown that excessive intake of high-fat diets increases the risk for overweight and obesity [2,3]. Increased fat intake in pre-adolescent children has been associated with subclinical inflammation, dyslipidemia, systemic insulin resistance and elevated blood pressure [4,5]. Obesity in children is also the major risk factor for development of pediatric non-alcoholic fatty liver disease (pNAFLD), defined histologically as $\geq 5\%$ of hepatocytes containing macrovesicular lipid droplets [6,7]. Up to 10% of children with pNAFLD develop non-alcoholic steatohepatitis (NASH), characterized by periportal lymphocytic infiltration, portal necrosis and

fibrosis [6,7]. However, few studies have examined the role of altered metabolism in the development of fatty liver disease in obese children.

Adipose tissue functions as a critical source of biologically active adipokines, such as tumor necrosis factor α (TNF- α), interleukin 6, adiponectin, leptin and resistin to regulate energy balance, glucose homeostasis, insulin sensitivity and lipid utilization [8]. Adiponectin is the most abundant adipokine in the circulation and has been shown to improve insulin sensitivity by increasing energy expenditure as the result of activation of adenosine monophosphate (AMP) kinase and of peroxisome proliferator-activator receptor- α (PPAR- α) signaling to influence fatty acid β - and ω -oxidation in both liver and skeletal muscle [9,10]. Adiponectin knockout mice fed a high-fat diet develop dyslipidemia and severe insulin resistance that can be reversed by viral-mediated adiponectin expression [11].

Moreover, supplementation with [12] or over-expression [13] of adiponectin in the obese *ob/ob* mouse fed a high-fat diet which has low serum adiponectin significantly decrease the accumulation of liver triglycerides and steatosis.

The regulation of circulating adiponectin levels appear to be both age-related and gender-specific, since children and females have

[☆] Financial Support: ARS CRIS #6251-51000-005-03S.

* Corresponding author. Arkansas Children's Nutrition Center, Little Rock, AR 72202, USA. Tel.: +1 501 364 2785; fax: +1 501 364 2818.

E-mail address: badgerthomas@uams.edu (T.M. Badger).

significantly greater levels than adults or males [14,15]. Unlike leptin, the circulating levels of adiponectin are reported to be reduced by 30–50% in obese adults, older children and adolescents as compared with their lean counterparts [16,17]. It has been suggested that the dysregulation of lipid metabolism resulting from reduced adiponectin action may be a causative factor and therefore be a potential biomarker of the “metabolic syndrome” in obesity [14,16,17]. The mechanisms involved in the regulation of adiponectin expression and secretion from adipose tissue are unclear, and the causative factor(s) that down-regulate adiponectin in obesity have yet to be identified.

On the other hand, the connection between adiponectin, insulin resistance, ectopic fat and obesity is not always clear. For example, a weaker association between serum adiponectin levels, and obesity was observed in younger children (age 2–6 years) [18] than in adults and older children. In addition, increased circulating adiponectin levels were reported in obese, spontaneously hypertensive rats [19], in obese C57BL/6J mice fed high-fat diets for 10 weeks [20] despite hyperinsulinemia and elevated tissue triglycerides, and in humans with anti-insulin receptor antibodies and extreme insulin resistance [21]. These studies point to a dissociation between serum adiponectin levels and energy homeostasis under various conditions. Moreover, few studies have examined the regulation of adiponectin signaling in relation to altered insulin sensitivity and lipid homeostasis specifically in obese children or young animals.

In adult animals, excessive caloric intake of high-fat diets produce elevated plasma triglycerides and non-esterified fatty acids (NEFA) leading to enhanced transport of fatty acids into the liver and skeletal muscles [22]. A high-fat diet was shown to increase hepatic expression of the fatty acid transporter FAT/CD36 gene [23], whereas the increased localization of FAT/CD36 protein in the sarcolemmal membrane without increases in gene expression has been suggested to contribute to ectopic lipid deposition in the muscle [24]. Ectopic fat deposition has been directly linked to the development of insulin resistance in skeletal muscle as the result of disruption of membrane translocation of the glucose transporter GLUT4 [25]. Impaired insulin signaling has in turn has been suggested to impair carbohydrate oxidation in muscle via increased pyruvate dehydrogenase kinase 4 transcription and inactivation of the pyruvate dehydrogenase complex as the result of decreased phosphorylation of Akt and of the downstream forkhead protein transcription factors FoxO1 and FoxO3 [26]. In the liver, insulin resistance has been shown to increase glucose production through de-repression of glucose 6-phosphatase and phosphoenolpyruvate carboxykinase also as the result of disrupted Akt and FoxO1 phosphorylation [27]. FoxO1 signaling in the liver has also been suggested to contribute to the development of hepatic steatosis in the face of insulin resistance as a result of a positive feedback on Akt phosphorylation via suppression of the Akt-inhibitory regulator Trb3 resulting in reduced fatty acid oxidation and increased triglyceride synthesis [28]. However, the contributions of adiponectin-mediated signaling relative to enhanced fatty acid transport and alterations in Akt-FoxO signaling in development of ectopic fat deposition and insulin resistance resulting from pediatric obesity are not well explored.

In the current study, we used a rat model in which excessive caloric intake of a high-fat diet was achieved by total enteral nutrition. This produced serological and histological features of clinical obesity, such as elevated adiposity, hepatosteatosis, dyslipidemia and hyperinsulinemia but resulted in increased rather than decreased serum adiponectin. The results (1) suggest that increased fatty acid transport is an early event in response to overfeeding a high-fat diet during development and leads to ectopic fat deposition, (2) demonstrate tissue-specific differences in the response of Akt-FoxO signaling to hyperinsulinemia following the development of pediatric obesity and (3) demonstrate that both ectopic fat deposition and hyperinsulinemia occur in the context of significantly elevated serum adiponectin

and adiponectin signaling in young animals. This latter point is particularly important in view of recent suggestions that hypo-adiponectinemia is a risk factor and useful biomarker of “metabolic syndrome” in children [15,16].

2. Methods

2.1. Animals and experimental protocol

Male Sprague–Dawley rats were purchased from Charles River Laboratories (Wilmington, MA, USA) and housed in an American Association for Accreditation of Laboratory Animal Care-approved animal facility. Protocols for animal maintenance and experimental treatments were conducted in accordance with the ethical guidelines for animal research established and approved by the Institutional Animal Care and Use Committee at the University of Arkansas for Medical Sciences. Rats were delivered at age postnatal day (PND) 24, were allowed to acclimate to the facility overnight, had intragastric cannulae surgically inserted as previously described [29], were placed in individual metabolism cages and were allowed to recover overnight with ad libitum access to drinking water. The animals were weighed and randomly distributed to experimental feeding groups.

Starting at PND26, rats were fed by total enteral nutrition (TEN) using a diet containing 43% of the calories as fat, 26% as protein and 33% carbohydrate (Table 1). The diet was formulated to mimic the general composition of the pediatric population [30]. In preliminary studies using cannulated rats having ad libitum access to standard food pellets (Tek-Lad, #8640) and rats fed by TEN, we empirically determined the daily caloric intake required for the TEN high-fat diet to match the body weight gains of pellet-fed rats (data not shown). No differences in body weights, adiposity, or serum concentrations of insulin or adiponectin were observed between animals weight-matched and fed standard food pellets (ad libitum), a low-fat TEN diet or a high-fat TEN diet (data not shown). In the current study, animals in the control group were fed the high-fat diet TEN diet at the caloric level to match ad libitum chow feeding and the overfed group was fed 25% more total diet than the control group. Thus herein, we focus on the metabolic and pathological effects of excessive caloric intake of a high-fat diet as a mediator of pediatric obesity.

Body composition of animals ($n=5$ per group) was assessed at PND38 and PND49 by nuclear magnetic resonance (NMR) (Echo Medical Systems, Houston, TX, USA) in unanesthetized animals, and the percentage of whole body fat and lean mass was determined and normalized to body weights. At PND48, two rats per group underwent X-ray computed tomography (CT) scanning (LaTheta LCT-100, Echo Medical Systems, Houston, TX, USA) under light isoflurane anesthesia. At PND50, animals were fasted overnight, euthanized and decapitated to collect trunk blood. The abdominal and gonadal fat pads were dissected, weighed and immediately frozen and stored at -70°C . Serum was collected and stored at -20°C until analyzed. Livers were removed and portions preserved both in formalin for paraffin embedding and in Optimal Cutting Temperature (OCT) Compound (Thermo Scientific) for subsequent histological analysis. Gastrocnemius muscles were dissected, preserved in OCT as well as snap frozen in liquid nitrogen, and stored at -70°C until analyzed. Lipid droplet formation was assessed by Oil Red O staining of OCT-preserved liver and muscle sections as described previously [28] and random fields from digitally captured images at $200\times$ magnification from each liver were quantified using the MCID Elite Software (GE Healthcare, Chalfont St. Giles, UK) linked to an Olympus Bx50 microscope.

2.2. Biochemical analyses

Serum NEFA was measured using the NEFA-C kit (Wako Chemicals, Richmond, VA, USA). Serum triglycerides and glucose levels were measured with Triglyceride Reagent and the Glucose Reagent (Synermed, Westfield, IN, USA) using the Cal II Calibration kit for comparison to standard curves. Serum insulin, leptin and adiponectin concentrations were measured using rat-specific ELISA kits from Linco Research (St. Charles, MO, USA) according to the manufacturer's protocols and recommended serum dilutions as necessary. Serum testosterone concentrations were measured using radioimmunoassay with a kit from Diagnostic System Laboratories (Webster, TX, USA). Serum alanine aminotransferase (ALT) activities were measured spectrophotometrically in a

Table 1
Macronutrient composition of the high-fat diet

	% kcal
Protein ^a	26
Fat ^b	41
Carbohydrate ^c	33
Vitamins/minerals ^d	-

^a Casein.

^b Corn oil (43%) and milk fat (57%).

^c Dextrose (79%), maltodextrin (19%), lactose (2%).

^d Added to meet or exceed the National Research Council recommended levels for the growing rat.

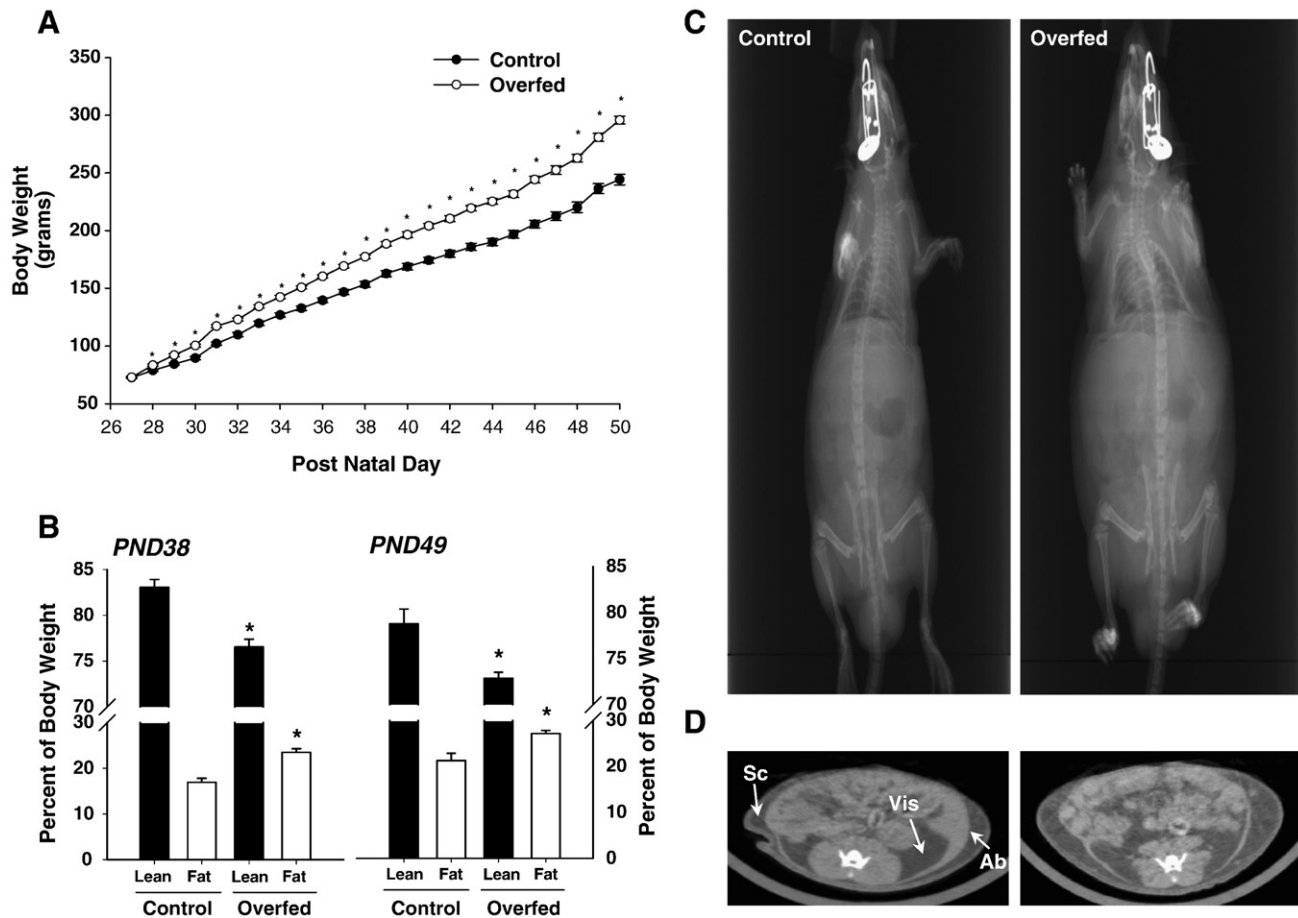


Fig. 1. Body weights and body composition of young rats overfed a high-fat diet. (A) Daily body weights of male rats fed the control high-fat diet (Control, black squares, $n=8$) or 25% more calories (Overfed, open circles, $n=10$) from PND27 to PND50. Data are expressed as mean \pm S.E.M. ($*P<.005$ versus Control using a Student's *t*-test). (B) Body composition of fat mass and lean mass as determined by NMR of control and overfed groups expressed as a percent of body weight at PND38 and PND49 ($*P<.05$ versus control, $n=5$ per group). (C, D) Representative CT scans at PND48 of control and overfed groups. A scout view (C) of the entire rat, and a transverse slice view (D) of representative rats are depicted. Sc, subcutaneous adipose tissue; Vis, visceral adipose tissue; Ab, abdominal wall.

standard 1 cm cuvette using the Infinity ALT reagent (Thermo Electron, Waltham, MA, USA) according to the manufacturer's protocol. Liver triglycerides were extracted from 250 mg of tissue, resuspended in acetone:water (2:1) solution and assayed as described above. For immunoblot analyses, total tissue lysates were prepared using RIPA buffer (25 mM Tris-Cl, 150 mM NaCl, 1% Nonidet P-40, 1% deoxycholate, 0.1% SDS, and 2 mM EDTA) supplemented with phosphatase inhibitors (Phosphatase Inhibitor Cocktails I and II, Sigma Chemical, St. Louis, MO, USA) and protease inhibitors. Proteins were resolved using an sodium dodecyl sulfate-polyacrylamide gel electrophoresis mini-gel apparatus and transferred to phenylmethane sulfonyl fluoride (PVDF) membranes. Nonspecific protein binding was blocked using 5% (w/v) non-fat dry milk in Tris-buffered saline containing 0.1% Tween-20 (TBS-Tween), and diluted antibodies were incubated overnight at 4°C. After washing with TBS-Tween, proteins were detected using horseradish peroxidase-conjugated secondary IgG (Santa Cruz Biotechnology, Santa Cruz, CA, USA) diluted 1:10,000 in TBS-Tween containing 5% non-fat dry milk. Antibody complexes were visualized using the ECL Plus reagent (Amersham/GE Healthcare) and detected using autoradiography. Immunodensitometry was performed by densitometry and analyzed using the QuantityOne software (BioRad, Hercules, CA, USA).

2.3. Liver tissue nuclear extracts

Nuclear-specific proteins were isolated from liver and muscle samples using the Nuclear Extract Kit (Active Motif, Carlsbad, CA, USA) according to the manufacturer's protocols. Briefly, 100 mg of frozen liver were homogenized in hypotonic buffer supplemented with protease and phosphatase inhibitor with 20 strokes of a ground-

glass homogenizer. Cells were allowed to lyse on ice and the unbroken cells and nuclei pelleted with centrifugation. Remaining intact cells were lysed with an additional aliquot of hypotonic buffer and the intracellular protein fraction separated by centrifugation. Proteins from intact nuclei were extracted using 50 μ l of lysis buffer supplemented with protease and phosphatase inhibitors for 30 min on ice followed by removal of the insoluble debris with centrifugation. Isolated nuclear proteins were quantitated as described above and stored at -70°C until used in FoxO1 Western blot analyses.

2.4. Subcellular fractionation of muscle tissue

Both the intracellular compartment and the membrane fraction of gastrocnemius muscle samples were obtained. Frozen tissues were homogenized in ice-cold buffer containing 20 mM Tris-HCl pH 7.5, 2 mM EDTA, 0.5 mM EGTA, 330 mM sucrose, 1 mM

Table 2
Characteristics of rats TEN-fed high-fat diets in the control and overfed groups

	Control ^b	Overfed ^b	<i>P</i> value ^c
Body weight (g)	244.3 \pm 4.6	295.8 \pm 3.3	<.001
% Liver weight ^a	5.12 \pm 0.15	5.38 \pm 0.17	.300
% Gonadal fat ^a	1.14 \pm 0.06	1.54 \pm 0.16	.022
% Abdominal fat ^a	1.47 \pm 0.12	2.10 \pm 0.17	.003
% Kidney weight ^a	0.86 \pm 0.02	0.91 \pm 0.06	.510
Total fat mass (grams)	48.01 \pm 4.32	72.28 \pm 4.90	.001
Body length (cm)	19.96 \pm 0.31	20.34 \pm 0.21	.304
Liver triglycerides (μ g/mg protein)	2.21 \pm 0.29	4.04 \pm 0.43	.008

^a Data represent the percentage of body weights.

^b Data represent mean \pm S.E.M. of six animals per group.

^c $P < .05$ is considered significant.

polyvinylidene difluoride (PMSF) and supplemented with phosphatase inhibitors (Phosphatase Inhibitor Cocktails I and II, Sigma Chemical) and protease inhibitors and centrifuged for 10 min at 1000×g at 4°C to remove debris and particulate material. The supernatants were transferred to ultracentrifuge tubes and centrifuged at 40,000×g for 1 h at 4°C. The samples representing the intracellular compartment were stored at –70°C, while membrane proteins in the pellets were solubilized with brief sonication in ice-cold homogenization buffer containing 1% Triton X-100, but lacking sucrose and centrifuged at 40,000×g for 1 hour at 4°C. Samples were frozen at –70°C until used in western blot analyses.

2.5. RNA isolation and real-time polymerase chain reaction

Total RNA was isolated from 25 mg of frozen liver or adipose tissue using the RNeasy mini columns (Qiagen, Valencia, CA) according to the manufacturer's recommended protocols. RNA quantity and quality were assayed spectrophotometri-

cally using the NanoDrop ND-100 apparatus (NanoDrop Technologies, Wilmington, DE, USA) and with the Experion RNA StdSens Chip on the Experion Automated Electrophoresis Station (BioRad). Total RNA (1 µg) was reverse-transcribed using the iScript Reverse Transcription kit (BioRad) and diluted to 10 ng/µl for use in real-time polymerase chain reaction (PCR). A total of 50 ng of cDNA was used for quantitative real-time PCR using the SYBR Green master mix (BioRad) with the MyiQ Real Time PCR Apparatus (BioRad). The relative quantities of the target genes were determined using serial 10-fold dilutions of cDNA to produce a standard curve. All gene-specific probes were designed using Primer Express Software, and the specific sequences are described in Ref. [31].

2.6. Statistical analysis

Data are expressed as the mean±S.E.M. Student *t* tests or analysis of variance followed by Student-Newman-Keuls post hoc comparisons were performed with

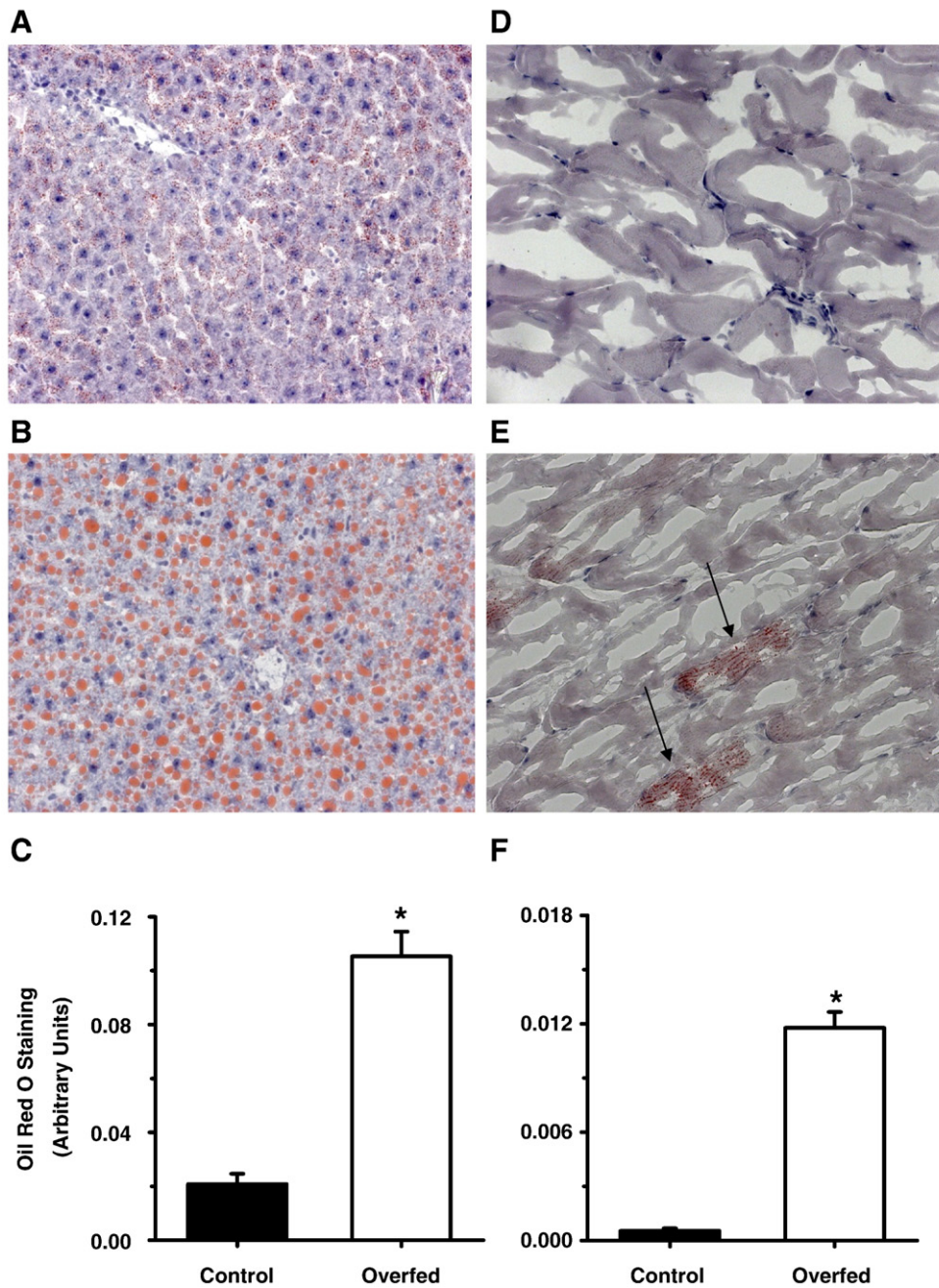


Fig. 2. Fat deposition in liver and gastrocnemius muscle of young rats overfed a high-fat diet. Representative Oil Red O staining of sections from liver (A, B) and gastrocnemius muscle (D, E) from control animals or overfed animals demonstrating significant hepatic steatosis (B) and intramyocellular lipid droplets (E, arrows) in response to excess caloric intake of a high-fat diet. Oil Red O staining of sections from liver (C) and muscle (F) were quantified using the MCID Elite Software from five digitally captured high power fields (200× magnification). Data are expressed as mean±S.E.M. of n=10 fields per group. Statistical differences were determined using the Student's *t* test. **P*<.001 versus the control group.

SigmaStat Version 3.3 (Systat Software, San Jose, CA, USA) software where appropriate. Calculated P values ≤ 0.05 were considered significant. Graphical representation of the data was performed using SigmaPlot Version 10.

3. Results

3.1. Effects of overfeeding a high-fat diet on body weight and adiposity

The mean body weight gain of the control group over the entire study was 7.2 ± 0.10 g/day. Providing 25% excess calories resulted in higher ($P < 0.05$) weight gains (9.1 ± 0.13 g/day) and 21% more body weight by PND50 (244.3 ± 4.6 versus 295.8 ± 3.3 g, $P < 0.001$) (Fig. 1A, Table 2). To examine changes in adiposity, the fat and lean masses were measured at PND38 and PND49 using NMR (Fig. 1B) in unanaesthetized rats. At PND38, there was a 38% increase ($P < 0.006$) in fat mass as a percentage of body weight in the overfed group, and by PND49 the overfed animals had 62% more fat mass than the control group ($P < 0.009$). In representative CT scans at PND48 (Fig. 1C), the whole animal radiogram showed increased body fat, and in the transverse cross-sectional images of abdominal regions, the overfed rat had qualitative increases in both abdominal and subcutaneous fat depots (Fig. 1D).

3.2. Overfeeding a high-fat diet produces ectopic fat disposition in liver and skeletal muscle

Liver and muscle tissue sections were stained with Oil Red O to determine ectopic lipid deposition and the degree of staining was quantitated by digital histomorphometry. In the control group, mild microsteatosis appeared throughout the liver (Fig. 2A), whereas lobular and periportal hepatocellular macrosteatosis was evident in liver of the overfed animals (Fig. 2B). Quantitative measurement of tissue Oil Red O staining confirmed a fivefold increase ($P < 0.001$) in the accumulation of lipid droplets in the liver (Fig. 2C). The total tissue triglycerides content was higher ($P < 0.008$) in liver of the overfed animals (Table 2). We also examined Oil Red O-stained sections of gastrocnemius muscle and observed a lipid droplet accumulation pattern that differed from that of liver. Overfeeding resulted in clusters of isolated intramyocellular lipid droplets in the overfed group rather than the more uniform distribution seen in the liver. Overfed rat muscle had greater fat accumulation ($P < 0.001$) (Fig. 2D–F, arrows).

3.3. Effects of overfeeding a high-fat diet on serum adiponectin and insulin

Adiponectin levels were increased ($P < 0.005$) from 24.6 ± 1.9 $\mu\text{g/ml}$ (controls) to 46.3 ± 5.9 $\mu\text{g/ml}$ (overfed), as did leptin concentrations (Table 3). These effects correlated with increased ($P < 0.001$) total fat mass (Table 2). Overfeeding led to a sevenfold increase (Table 3) of circulating insulin concentrations compared with controls, from 2.2 ± 0.2 to 14.0 ± 2.5 ng/ml ($P < 0.001$), suggestive of systemic insulin resistance. Serum concentrations of total triglycerides and NEFA were

Table 3
Serum measurements of endocrine markers in the control and overfed groups

	Control ^a	Overfed ^a	P value ^b
Glucose (mg/dl)	40.6 ± 1.2	44.1 ± 1.3	.066
Insulin (ng/ml)	2.2 ± 0.2	14.0 ± 2.5	<.001
Triglyceride (mg/dl)	85.2 ± 6.9	160.7 ± 16.5	.006
NEFA (mM)	$6.5 \pm 0.$	16.8 ± 1.8	<.001
ALT (U/L)	44.2 ± 2.0	67.1 ± 4.6	.001
Leptin (ng/ml)	13.2 ± 1.7	33.4 ± 2.3	<.001
Adiponectin ($\mu\text{g/ml}$)	24.6 ± 1.9	46.3 ± 5.9	.004
Serum Testosterone (ng/ml)	0.7 ± 0.22	0.41 ± 0.17	.450

^a Data represent the mean \pm S.E.M. of six animals per group.

^b $P < 0.05$ is considered significant.

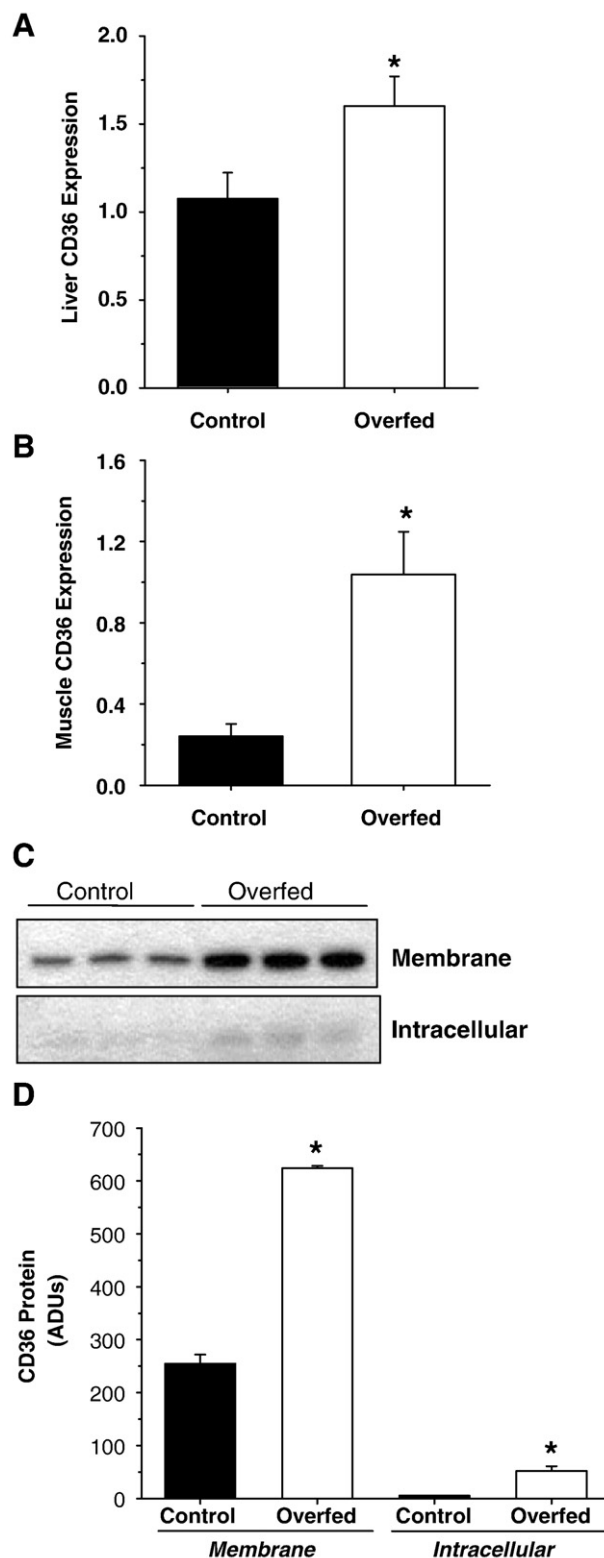


Fig. 3. FAT/CD36 expression in liver and gastrocnemius muscle in young rats overfed a high-fat diet. Total RNA isolated from liver (A) and gastrocnemius muscle (B) was reverse-transcribed into cDNA, and the expression of FAT/CD36 was determined. Expression values were normalized to the expression of cyclophilin A as an internal control. Data are expressed as mean \pm S.E.M. ($n = 6$ per group). Statistical differences were determined using the Student's t test. * $P < 0.008$ versus the control. (C) Proteins (25 μg) from the subcellular fractionation of gastrocnemius muscle representing the membrane and intracellular compartments were assayed for FAT/CD36 by Western blot analysis. (D) Immunodetection of FAT/CD36 protein in muscle.

increased ($P<.05$) in the overfed group (Table 3). Additionally, serum ALT activities were increased in the overfed group ($P<.001$) (Table 3) suggesting mild hepatic injury.

3.4. Effect of overfeeding on fatty acid transport in liver and muscle tissues

The high levels of serum triglycerides and NEFA led us to examine the expression of the scavenger receptor FAT/CD36, known to be involved in the uptake of long chain fatty acids into liver and muscle [22–24]. Quantitative PCR analyses of FAT/CD36 (Fig. 3A and B) demonstrated increased expression in liver (Fig. 3A, $P<.05$) and muscle ($P<.05$, Fig. 3B) in response to overfeeding. In muscle (Fig. 3C and D), the presence of FAT/CD36 in the membrane fraction was also increased ($P<.05$), with little CD36 localizing to the intracellular compartment. The up-regulation of FAT/CD36 suggests enhanced

fatty acid import contributed to ectopic fat storage in liver and muscle of the overfed animals.

3.5. Effects of overfeeding on hepatic and skeletal muscle Akt-FoxO signaling

Increases in hepatic triglycerides have been associated with development of hepatic insulin resistance in diet-induced obesity in adults [32,33]. We observed increased phosphorylation of Akt-serine⁴⁷³ (Fig. 4A and B) in liver, consistent with an increase in hepatic insulin signaling in response to the increased serum insulin. When FoxO1 is phosphorylated by Akt, it has been shown to be excluded from the nucleus and tagged for degradation [34]. Hepatic nuclear FoxO1 content decreased ($P<.05$) in the overfed animals suggesting that phospho-Akt signaling in response to insulin was intact (Fig. 4A and B). Thus, the hepatic Akt-dependent insulin

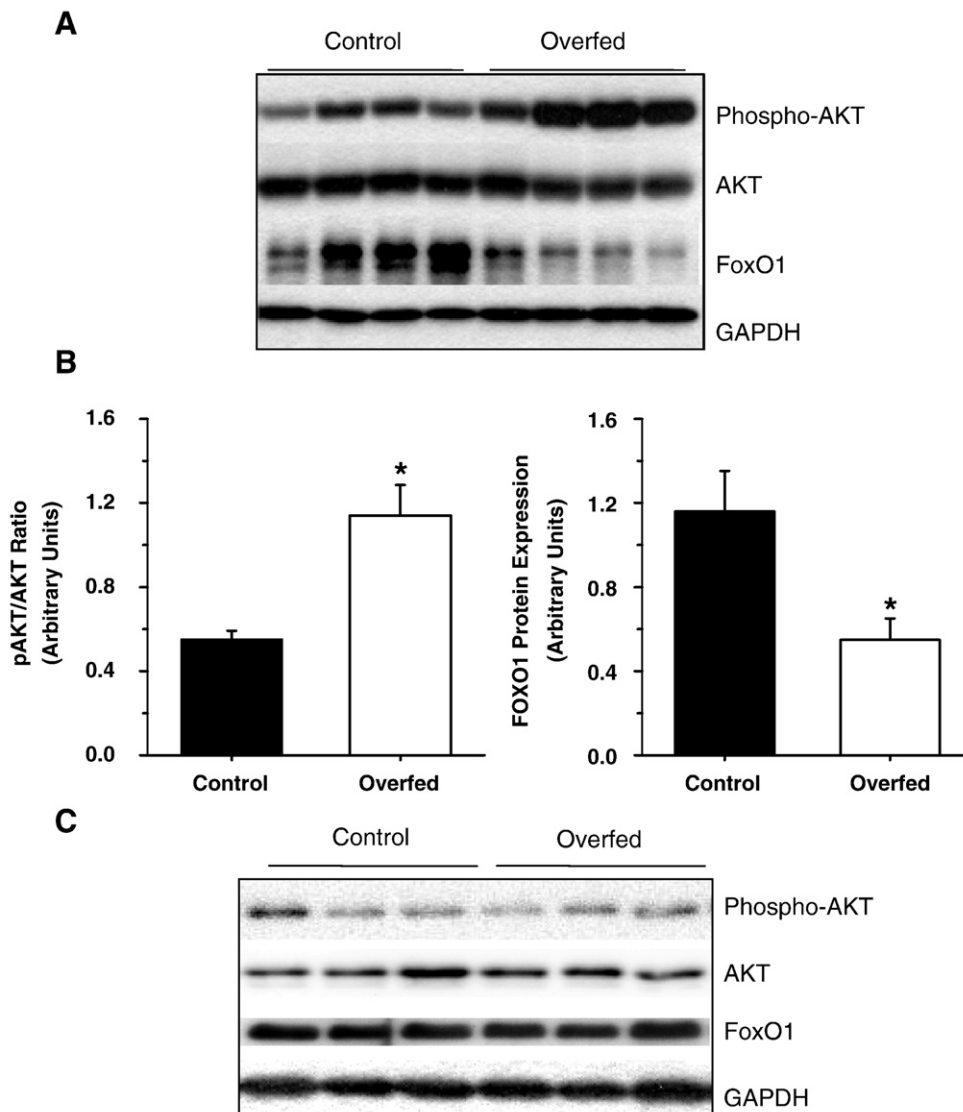


Fig. 4. Phospho-Akt and FoxO1 in liver and gastrocnemius muscle of young rats overfed and high-fat diet. (A) The protein expression and phosphorylation status of Akt (Ser⁴⁷³) in whole cell extracts of livers from control and overfed groups were determined using Western blot analysis using specific antibodies. GAPDH expression was used as a protein loading control. To measure Akt activity, the protein expression of FoxO1 was determined in nuclear extracts from liver tissues. (B) Data from the densitometric analysis of the FoxO1 content and phospho-Akt/Akt ratio are expressed as mean±S.E.M. of $n=4$ per group. (C) The protein expression and phosphorylation status of Akt (Ser⁴⁷³) in whole cell extracts and protein expression of FoxO1 in nuclear extracts from gastrocnemius muscles from control and overfed groups were determined using Western blot analysis. GAPDH expression was used as a protein loading control. Statistical significance was determined using the Student's *t* test. * $P<.03$ versus the control group.

signaling pathway in the liver was maintained in the overfed group. This suggests that hepatic insulin sensitivity was preserved despite the development of hepatosteatosis. We also examined Akt-dependent insulin signaling in the gastrocnemius muscle as an indices of insulin sensitivity in skeletal muscle and found no changes of Akt-serine⁴⁷³ phosphorylation or nuclear FoxO1 expression (Fig. 4C) in the overfed group. This suggests a blunted response to hyperinsulinemia in the gastrocnemius muscle, consistent with insulin resistance in this tissue.

3.6. Effects of overfeeding a high-fat diet on adipose tissue adiponectin and TNF- α expression

Since adipose tissue is the main source of adiponectin, we isolated RNA from abdominal adipose tissue to determine the expression level of adiponectin in response to overfeeding. Quantitative PCR analysis (Fig. 5A) demonstrated that adiponectin expression did not differ significantly between diet groups. The inflammatory cytokine TNF- α has been implicated in the transcriptional down-regulation of adiponectin in response to chronic inflammation [35]. We observed no change in adipose tissue TNF- α expression (Fig. 5B) in the overfed animals. Together, these data suggest that the high fat mass in the overfed animals did not result in increased inflammation, and the elevated serum adiponectin in the overfed animals resulted from normal secretion of a greater fat mass.

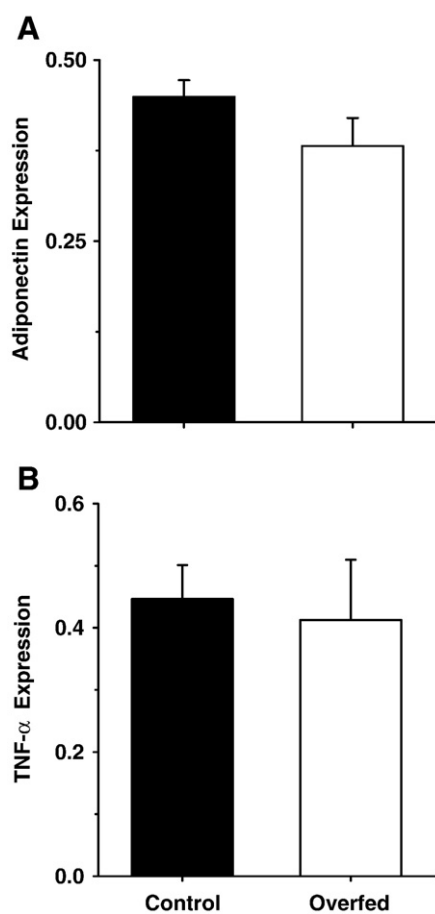


Fig. 5. Adiponectin and TNF- α expression in adipose tissue young rats overfed a high-fat diet. The mRNA expression levels of adiponectin (A) and TNF- α (B) were determined in abdominal fat tissue using quantitative PCR. Expression values were normalized to the expression of cyclophilin A as an internal control. Data are expressed as mean \pm S.E.M. ($n=6$ per group). No statistical differences between groups for either gene analyzed were determined using the Student's t test.

3.7. Effects of overfeeding on hepatic and skeletal muscle adiponectin receptors and AMP kinase activation

Adiponectin receptor signaling has been shown to activate AMP kinase through phosphorylation of threonine¹⁷² [36]. Western blot analysis revealed increased hepatic and muscular phospho-AMP kinase in overfed rats without an increase in total AMP kinase protein (Fig. 6A and B). This suggests that both liver and muscle tissues remained sensitive to adiponectin. In liver, the expression of the adiponectin receptor AdipoR1 was increased, while AdipoR2 was unchanged (Fig. 6C). Similarly, in gastrocnemius muscle, both AdipoR1 and AdipoR2 were up-regulated in response to overfeeding (Fig. 6C), supporting the hypothesis that adiponectin signaling in liver and muscle remained intact.

3.8. Effects of overfeeding a high-fat diet on fatty acid oxidation

Adiponectin has been reported to mediate the up-regulation of β -oxidation of fatty acids and decrease lipid content in liver and muscle [9]. Overfeeding led to increased ($P<.05$) mRNA levels of PPAR- α , a key nuclear receptor that may also be up-regulated by adiponectin signaling [9,10] in liver and muscle (Fig. 7A and D). Acyl-CoA oxidase (ACO) is involved in peroxisomal β -oxidation, and carnitine palmitoyl transferase-I (CPT-I) is a mitochondrial fatty acid transporter. Genes for these proteins are PPAR- α -dependent and they were also induced in the overfed group, suggesting increased liver and muscle fatty acid oxidation (Fig. 7B-F).

4. Discussion

In the current study, we used total enteral nutrition to control diet composition and caloric intake of weanling rats. Feeding a high-fat diet at caloric levels greater than those required for normal growth produced a phenotype similar to that reported in obese children, characterized by a high body fat content, hepatosteatosis and intramyocellular triglyceride accumulation in skeletal muscle and hyperinsulinemia [2,3]. However, one aspect, circulating adiponectin concentrations, differed substantially from some previously published reports.

Adiponectin has been linked to the maintenance of energy homeostasis in insulin sensitive tissues, such as liver and muscle. A decrease in adiponectin secretion has been implicated as a potential causative factor in the development of ectopic fat deposition and insulin resistance [15,16]. The increase serum adiponectin concentrations observed in the current study are in contrast to several previous reports where adiponectin was found to be significantly lower with obesity [15,16,37,38]. In adult humans, hypoadiponectinemia correlated with obesity-related insulin resistance [38] and Type 2 diabetes [39]. Reduced adiponectin was also reported to be a major feature and an early risk factor in the pediatric population for the development of NAFLD and NASH [40]. However, other studies in children and adolescents have not found a strong association between adiponectin levels, insulin resistance and obesity. For example, lower serum adiponectin levels were not associated with greater insulin resistance in obese adolescents [1], and only a weak association between plasma adiponectin and obesity was reported in 2–6-year olds [18]. Moreover, in another study of obese children and adolescents, Winer et al. [41] reported no significant association between HOMA (the Homeostasis Model Assessment of insulin resistance); the prevalence of impaired glucose tolerance or the odds ratio for meeting the criteria for metabolic syndrome with serum adiponectin concentrations after controlling for possible confounders, despite a positive association between serum adiponectin and calculated whole body insulin sensitivity index. Further evidence for the dissociation of insulin resistance from serum adiponectin was reported in a study of

individuals with extreme insulin resistance resulting from genetically defective insulin receptors or acquired anti-insulin receptor antibodies with fourfold higher serum adiponectin as compared to normals [21].

Data presented herein are in better agreement with those of Barnea et al. [42] who observed no serum adiponectin deficiency in animals fed a high-fat diet (42% of the calories as fat) for 4 months despite hyperinsulinemia and moderate increases in serum and tissue triglycerides. Similarly, Bullen et al. [20] observed a positive correlation rather than a negative correlation between adiponectin expression and increased adiposity in obese C57BL/6J mice fed a high-

fat diet for 10 weeks, though adiponectin levels became lower in the high fat group by 18 weeks.

Adiponectin acts through AdipoR1 and AdipoR2 to activate the AMP-dependant kinase. This in turn stimulates PPAR- α -dependent gene expression in insulin-sensitive tissues to increase expression of critical components of the peroxisomal and mitochondrial fatty oxidation pathways [43,44]. In the overfed group of the current study, phosphorylation of AMP kinase was significantly increased, and there was up-regulation of the mitochondrial fatty acid transporter CPT-1 and a key enzyme involved in peroxisomal β -oxidation, ACO. These effects are consistent with the elevated serum adiponectin

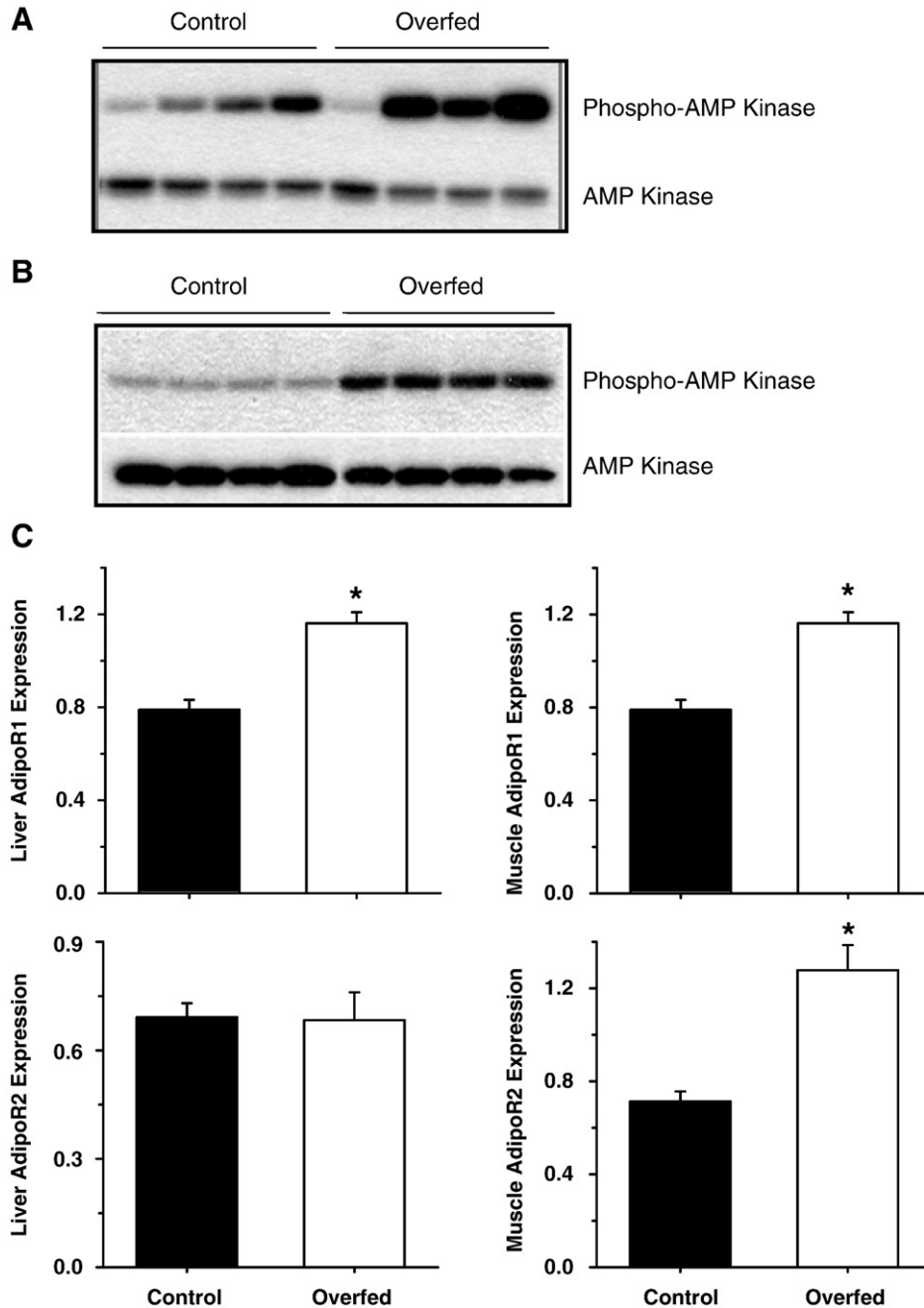


Fig. 6. AMP kinase phosphorylation and adiponectin receptors AdipoR1 and AdipoR2 liver and gastrocnemius muscle in young rats overfed a high-fat diet. The protein expression and phosphorylation of AMP kinase (Thr¹⁷²) in whole cell extracts from liver (A) and gastrocnemius muscle (B) were determined using Western blot analysis using specific antibodies. GAPDH expression was used as a protein loading control. Total RNA isolated from liver (C, left panels) and muscle (C, right panels) was reverse transcribed into cDNA, and the expression of AdipoR1 and AdipoR2 were determined with quantitative PCR. Expression values were normalized to the expression of cyclophilin A as an internal control. Data are expressed as mean \pm SEM (N=6 per group). Statistical differences were determined using the Student's *t* test. **P*<.001 versus the control group.

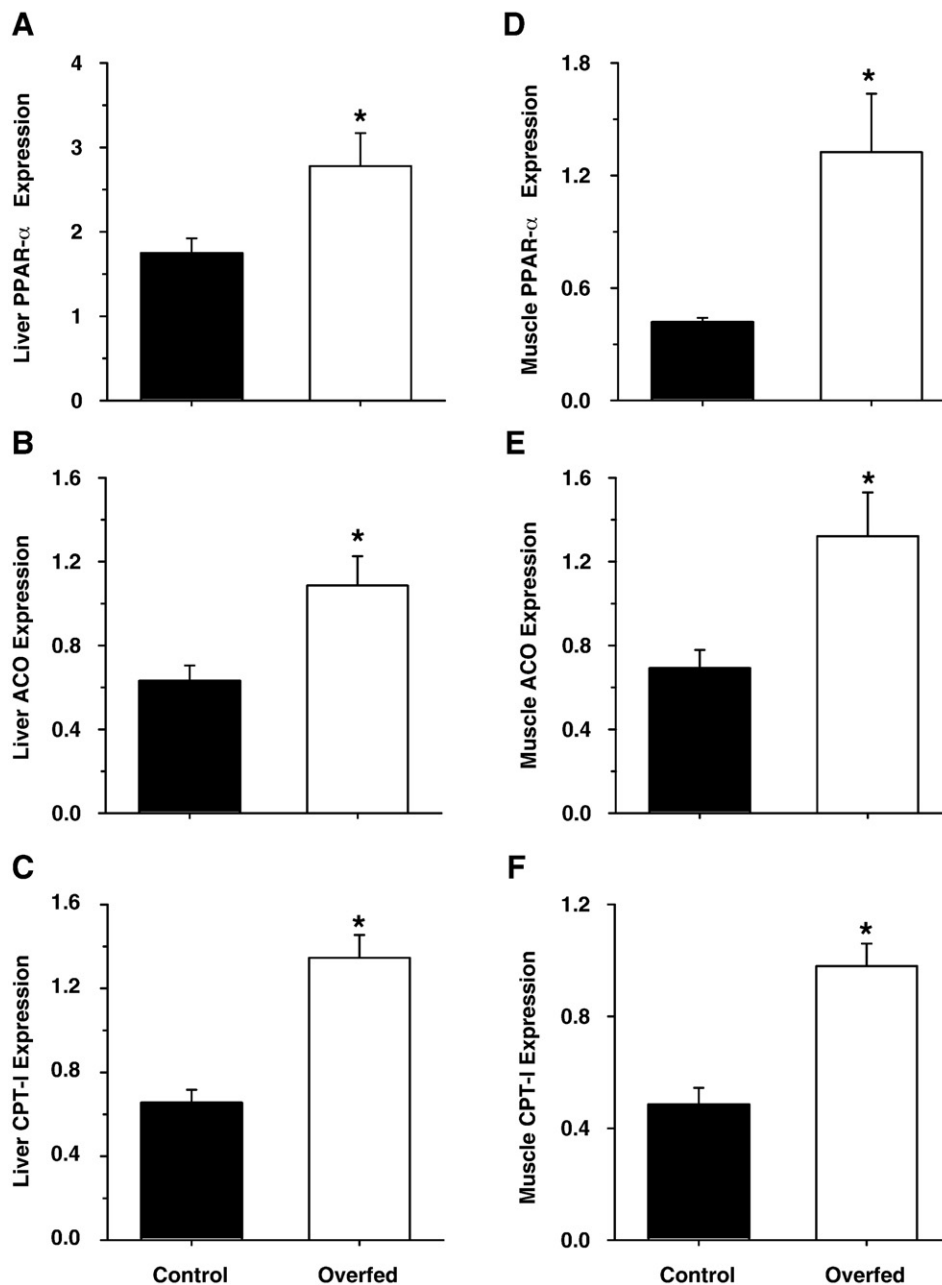


Fig. 7. Genes involved in fatty acid oxidation are increased in the liver and muscle of animals overfed a high-fat diet. The expression level of PPAR- α in liver (A) and muscle (D) was determined using quantitative PCR. Expression values were normalized to the expression of cyclophilin A as an internal control. Data are expressed as mean \pm S.E.M. ($n=6$ per group). Statistical differences were determined using the Student's t test. * $P<.001$ versus the control. The expression of ACO and CPT-1 in liver (B, C) and muscle (E, F) was determined with quantitative PCR and normalized to cyclophilin A as an internal control. Data are expressed as mean \pm S.E.M. ($n=6$ per group). Statistical differences were determined using the Student's t test. * $P<.001$ versus the control group.

concentrations and adiponectin-mediated signaling [9,45] and argue against adiponectin resistance as a mechanism contributing to hyperadiponectinemia. Proinflammatory cytokines, including TNF- α and IL-6, have been suggested to negatively regulate adiponectin expression [46], and low-level, chronic inflammation in the adipose tissues has been observed in obese individuals [47]. This suggests that down-regulation of adiponectin reported in obese patients may be a result of chronic inflammation. In the current study, the lack of TNF- α activation in the adipose tissue of the overfed animals suggests an absence of inflammation and could partially explain the increased adiponectin levels in young obese rats. Since pre-adipocytes from young rodents have greater fatty acid-induced differentiation and are

less susceptible to lipotoxicity than pre-adipocytes from adult animals [48], expansion of adipose depots in response to excess caloric intake may result primarily from increased adipogenesis in early development. In older obese animals and adult animal models of NASH [47,48], dysfunctional fatty acid metabolism in the adipose tissue leads to increased apoptosis and chronic inflammation. Thus, the combination of low inflammation and a high rate of adipogenesis in young animals could favor higher serum adiponectin. These data may provide insights into how and why overweight or obese children have a somewhat different clinical picture than adults.

Even though young rats overfed high-fat diets developed marked hyperinsulinemia, plasma glucose levels remained unaltered. These

data are consistent with the development of systemic insulin resistance which is compensated for by excessive pancreatic insulin secretion. Surprisingly, analysis of hepatic Akt-FoxO1 signaling revealed increased Akt phosphorylation and reduced nuclear FoxO1 expression consistent with suppression of FoxO signaling, a normal response to elevated serum insulin and retention of insulin sensitivity. The retention of insulin sensitivity might contribute to increased hepatic triglyceride accumulation, since enhanced Akt signaling results in activation of sterol regulatory binding protein 1c, a transcription factor responsible for increased expression of genes involved in de novo hepatic fatty acid synthesis such as fatty acid synthase and acyl-CoA carboxylase [49]. These data differ from those reported in diabetic models such as the *db/db* mouse and in adult mice fed high-fat diets, where serum glucose is elevated, hepatic insulin signaling is impaired and hepatic FoxO signaling is activated [50,51]. In these mouse models, introduction of dominant inhibitory FoxO1 or FoxO1 knockdown has been reported to decrease the serum glucose values to those of non-diabetic or lean mice [50,51]. In contrast to the liver, no changes in Akt phosphorylation or nuclear FoxO1 expression were observed in skeletal muscle of young rats overfed the high-fat diet, despite the dramatic increase in serum insulin. This is consistent with development of insulin resistance in the muscle previously reported to be associated with accumulation of intramyocellular triglycerides both in humans and animal models [10,25,27]. Normalization of muscular Akt-FoxO signaling in the insulin-resistant muscle as a result of compensatory increases in serum insulin may be important to prevent muscle wasting and impairment of muscle carbohydrate oxidation which have been shown to be targets of this signaling pathway [26].

In summary, young rats overfed a high-fat diet developed obesity, ectopic fat deposition and changes in muscle insulin signaling consistent with peripheral insulin resistance and expressed pathological markers of pediatric NAFLD, despite increases in serum adiponectin and adiponectin-mediated up-regulation of fatty acid oxidation. In addition, fatty acid import via FAT/CD36 was increased and likely contributed to ectopic fat deposition in both the liver and muscle. These results, when combined with previously published data, demonstrate that ectopic fat deposition and hyperinsulinemia in developmental obesity can occur independent of serum adiponectin concentrations and adiponectin-mediated signaling. They further suggest a more important role for increased uptake of fatty acids in ectopic fat deposition and development of endocrine disorders during early development. The elucidation of the metabolic mechanisms altered by over-consumption of high-fat diets in young animals may lead to a better understanding of how to prevent or treat metabolic sequelae of childhood obesity.

Acknowledgments

The authors wish to thank Matt Ferguson, Tammy Dallari and Trae Pittman for technical assistance with surgical procedures and animal handling. We also wish to thank Rachel Nicholson and Jamie Vantrease for technical assistance.

References

- [1] Papatheou D, Rousso I, Mavromichalis I. Update on non-alcoholic fatty liver disease in children. *Clin Nutr* 2007;26:409–15.
- [2] Johnson L, Mander AP, Jones LR, Emmett PM, Jebb SA. Energy-dense, low-fiber, high-fat dietary pattern is associated with increased fatness in childhood. *Am J Clin Nutr* 2008;87:846–54.
- [3] McNaughton SA, Ball K, Mishra GD, Crawford DA. Dietary patterns of adolescents and risk of obesity and hypertension. *J Nutr* 2008;138:364–70.
- [4] Syrenicz A, Garanty-Bogacka B, Syrenicz M, Gebala A, Walczak M. Low-grade systemic inflammation and the risk of type 2 diabetes in obese children and adolescents. *Neuro Endocrinol Lett* 2006;27:453–8.
- [5] Aeberli I, Beljean N, Lehmann R, l'Allemand D, Spinass GA, Zimmermann MB. The increase of fatty acid-binding protein aP2 in overweight and obese children: interactions with dietary fat and impact on measures of subclinical inflammation. *Int J Obes (Lond)* 2008;32:1513–20.
- [6] Schwimmer JB, Behling C, Newbury R, Deutsch R, Nievergelt C, Schork NJ, et al. Histopathology of pediatric nonalcoholic fatty liver disease. *Hepatology* 2005;42:641–9.
- [7] Schwimmer JB. Definitive diagnosis and assessment of risk for nonalcoholic fatty liver disease in children and adolescents. *Semin Liver Dis* 2007;27:312–8.
- [8] Kershaw EE, Flier JS. Adipose tissue as an endocrine organ. *J Clin Endocrinol Metab* 2004;89:2548–56.
- [9] Yamauchi T, Nio Y, Maki T, Kobayashi M, Takazawa T, Iwabu M, et al. Targeted disruption of AdipoR1 and AdipoR2 causes abrogation of adiponectin binding and metabolic actions. *Nat Med* 2007;13:332–9.
- [10] Arner P. The adipocyte in insulin resistance: key molecules and the impact of the thiazolidinediones. *Trends in Endocrinol. Metab* 2003;14:137–45.
- [11] Nawrocki AR, Rajala MW, Tomas E, Pajvani UB, Saha AK, Trumbauer ME, et al. Mice lacking adiponectin show decreased hepatic insulin sensitivity and reduced responsiveness to peroxisome proliferator-activated receptor gamma agonists. *J Biol Chem* 2006;281:2654–60.
- [12] Xu A, Wang Y, Keshaw H, Xu LY, Lam KS, Cooper GJ. The fat-derived hormone adiponectin alleviates alcoholic and nonalcoholic fatty liver diseases in mice. *J Clin Invest* 2003;112:91–100.
- [13] Kim JY, van de WE, Laplante M, Azzara A, Trujillo ME, Hofmann SM, et al. Obesity-associated improvements in metabolic profile through expansion of adipose tissue. *J Clin Invest* 2007;117:2621–37.
- [14] Punthakee Z, Delvin EE, O'loughlin J, Paradis G, Levy E, Platt RW, et al. Adiponectin, adiposity, and insulin resistance in children and adolescents. *J Clin Endocrinol Metab* 2006;91:2119–25.
- [15] Asayama K, Hayashibe H, Dobashi K, Uchida N, Nakane T, Kodera K, et al. Decrease in serum adiponectin level due to obesity and visceral fat accumulation in children. *Obes Res* 2003;11:1072–9.
- [16] Kern PA, Di Gregorio GB, Lu T, Rassouli N, Ranganathan G. Adiponectin expression from human adipose tissue: relation to obesity, insulin resistance, and tumor necrosis factor- α expression. *Diabetes* 2003;52:1779–85.
- [17] Imhof A, Kratzler W, Boehm B, Meitinger K, Trischler G, Steinbach G, et al. Prevalence of non-alcoholic fatty liver and characteristics in overweight adolescents in the general population. *Eur J Epidemiol* 2007;22:889–97.
- [18] Cianflone K, Lu H, Smith J, Yu W, Wang H. Adiponectin, acylation stimulating protein and complement C3 are altered in obesity in very young children. *Clin Endocrinol (Oxf)* 2005;62:567–72.
- [19] Rodriguez A, Catalan V, Beceril S, Gil MJ, Mugueta C, Gomez-Ambrosi J, et al. Impaired adiponectin-AMPK signaling in insulin-sensitive tissues of hypertensive rats. *Life Sci* 2008;83:540–9.
- [20] Bullen Jr JW, Blüher S, Kelesidis T, Mantzoros CS. Regulation of adiponectin and its receptors in response to development of diet-induced obesity in mice. *Am J Physiol Endocrinol Metab* 2007;292:E1079–86.
- [21] Semple RK, Halberg NH, Burling K, Soos MA, Schraw T, Luan J, et al. Paradoxical elevation of high-molecular weight adiponectin in acquired extreme insulin resistance due to insulin receptor antibodies. *Diabetes* 2007;56:1712–7.
- [22] Memon RA, Fuller J, Moser AH, Smith PJ, Grunfeld C, Feingold KR. Regulation of putative fatty acid transporters and Acyl-CoA synthetase in liver and adipose tissue in *ob/ob* mice. *Diabetes* 1999;48:121–7.
- [23] Koonen DP, Jacobs RL, Febbraio M, Young ME, Soltys CL, Ong H, et al. Increased hepatic CD36 expression contributes to dyslipidemia associated with diet-induced obesity. *Diabetes* 2007;56:2863–71.
- [24] Holloway GP, Luiken JJ, Glatz JF, Spriet LL, Bonen A. Contribution of FAT/CD36 to the regulation of skeletal muscle fatty acid oxidation: an overview. *Acta Physiol (Oxf)* 2008;194:291–309.
- [25] Boden G, Shulman GI. Free fatty acids in obesity and type 2 diabetes: defining their role in development of insulin resistance and beta cell dysfunction. *Eur J Clin Invest* 2002;32:14–23.
- [26] Crossland H, Constantin-Teodosiu, Gardiner SM, Constantin D, Greenhaff PL. A potential role for Akt/FOXO signaling in both protein loss and the impairment of muscle carbohydrate oxidation during sepsis in rodent skeletal muscle. *J Physiol* 2008;586:5589–600.
- [27] Gross DN, Wan M, Birnbaum MJ. The role of FOXO in the regulation of metabolism. *Curr. Diabetes Rep* 2009;9:208–14.
- [28] Matsumoto M, Han S, Kitamura T, Accili D. Dual role of transcription factor FoxO1 in controlling hepatic insulin sensitivity and lipid metabolism. *J Clin Invest* 2006;116:2464–72.
- [29] Ronis MJ, Butura A, Sampey BP, Shankar K, Prior RL, Korourian S, et al. Effects of N-acetylcysteine on ethanol-induced hepatotoxicity in rats fed via total enteral nutrition. *Free Radic Biol Med* 2005;39:619–30.
- [30] McGloin AF, Livingstone MB, Greene LC, Webb SE, Gibson JM, Jebb SA, et al. Energy and fat intake in obese and lean children at varying risk of obesity. *Int J Obes Relat Metab Disord* 2002;26:200–7.
- [31] Baumgardner JN, Shankar K, Hennings L, Badger TM, Ronis MJ. A new model for nonalcoholic steatohepatitis in the rat utilizing total enteral nutrition to overfeed a high-polyunsaturated fat diet. *Am J Physiol Gastrointest Liver Physiol* 2008;294:G27–G38.
- [32] Deng QG, She H, Cheng JH, French SW, Koop DR, Xiong S, et al. Steatohepatitis induced by intragastric overfeeding in mice. *Hepatology* 2005;42:905–14.

- [33] Ota T, Takamura T, Kurita S, Matsuzawa N, Kita Y, Uno M, et al. Insulin resistance accelerates a dietary rat model of nonalcoholic steatohepatitis. *Gastroenterology* 2007;132:282–93.
- [34] Matsuzaki H, Daitoku H, Hatta M, Tanaka K, Fukamizu A. Insulin-induced phosphorylation of FKHR (Foxo1) targets to proteasomal degradation. *Proc Natl Acad Sci U S A* 2003;100:11285–90.
- [35] Araki S, Dobashi K, Kubo K, Yamamoto Y, Asayama K, Shirahata A. N-acetylcysteine attenuates TNF- α induced changes in secretion of interleukin-6, plasminogen activator inhibitor-1 and adiponectin from 3T3-L1 adipocytes. *Life Sci* 2006;79:2405–12.
- [36] Hawley SA, Davison M, Woods A, Davies SP, Beri RK, Carling D, et al. Characterization of the AMP-activated protein kinase kinase from rat liver and identification of threonine 172 as the major site at which it phosphorylates AMP-activated protein kinase. *J Biol Chem* 1996;271:27879–87.
- [37] Garcia-Ruiz I, Rodriguez-Juan C, Diaz-Sanjuan T, Martinez MA, Munoz-Yague T, Solis-Herruzo JA. Effects of rosiglitazone on the liver histology and mitochondrial function in ob/ob mice. *Hepatology* 2007;46:414–23.
- [38] Weyer C, Funahashi T, Tanaka S, Hotta K, Matsuzawa Y, Pratley RE, et al. Hypoadiponectinemia in obesity and type 2 diabetes: close association with insulin resistance and hyperinsulinemia. *J Clin Endocrinol Metab* 2001;86:1930–5.
- [39] Spranger J, Kroke A, Mohlig M, Bergmann MM, Ristow M, Boeing H, et al. Adiponectin and protection against type 2 diabetes mellitus. *Lancet* 2003;361:226–8.
- [40] Brooks NL, Moore KS, Clark RD, Perfetti MT, Trent CM, Combs TP. Do low levels of circulating adiponectin represent a biomarker or just another risk factor for the metabolic syndrome? *Diabetes Obes Metab* 2007;9:246–58.
- [41] Winer JC, Zern TL, Taksali SE, Dziura J, Cali AM, Wollschlaeger M, et al. Adiponectin in childhood and adolescent obesity and its association with inflammatory markers and components of the metabolic syndrome. *J Clin Endocrinol Metab* 2006;91:4415–23.
- [42] Barnea M, Shamay A, Stark AH, Madar Z. A high-fat diet has a tissue-specific effect on adiponectin and related enzyme expression. *Obesity (Silver Spring)* 2006;14:2145–53.
- [43] Varanasi U, Chu R, Huang Q, Castellon R, Yeldandi AV, Reddy JK. Identification of a peroxisome proliferator-responsive element upstream of the human peroxisomal fatty acyl coenzyme A oxidase gene. *J Biol Chem* 1996;271:2147–55.
- [44] Minnich A, Tian N, Byan L, Bilder G. A potent PPAR- α agonist stimulates mitochondrial fatty acid beta-oxidation in liver and skeletal muscle. *Am J Physiol Endocrinol Metab* 2001;280:E270–9.
- [45] Yoon MJ, Lee GY, Chung JJ, Ahn YH, Hong SH, Kim JB. Adiponectin increases fatty acid oxidation in skeletal muscle cells by sequential activation of AMP-activated protein kinase, p38 mitogen-activated protein kinase, and peroxisome proliferator-activated receptor- α . *Diabetes* 2006;55:2562–70.
- [46] Whitehead JP, Richards AA, Hickman IJ, Macdonald GA, Prins JB. Adiponectin—a key adipokine in the metabolic syndrome. *Diabetes Obes Metab* 2006;8:264–80.
- [47] Bastard JP, Maachi M, Lagathu C, Kim MJ, Caron M, Vidal H, et al. Recent advances in the relationship between obesity, inflammation, and insulin resistance. *Eur Cytokine Netw* 2006;17:4–12.
- [48] Guo W, Pirtskhalava T, Tchkonja T, Xie W, Thomou T, Han J, et al. Aging results in paradoxical susceptibility of fat cell progenitors to lipotoxicity. *Am J Physiol Endocrinol Metab* 2007;292:E1041–51.
- [49] He L, Marecki JC, Serrero G, Simmen FA, Ronis MJJ, Badger TM. Dose-dependent effects of alcohol on insulin signaling: Partial explanation for biphasic alcohol impact on human health. *Mol Endocrinol* 2007;21:2541–50.
- [50] Altomonte J, Richter A, Harbaran S, Suriawinata J, Nakae J, Thung SN, et al. Inhibition of Foxo1 function is associated with improved fasting glycemia in diabetic mice. *Am J Physiol Endocrinol Metab* 2003;285:E718–28.
- [51] Samuel VT, Choi CS, Phillips TG, Romanelli AJ, Geisler JG, Bhanot S, et al. Targeting foxo1 in mice using antisense oligonucleotide improves hepatic and peripheral insulin action. *Diabetes* 2006;55:2042–50.